

# Interactive Data Visualization with Multidimensional Scaling

Andreas BUJA <sup>1</sup>, Deborah F. SWAYNE <sup>2</sup>,  
Michael L. LITTMAN <sup>3</sup>, Nathaniel DEAN <sup>4</sup>,  
and Heike HOFMANN <sup>5</sup>

March 29, 2004

We discuss interactive techniques for multidimensional scaling (MDS) and a two systems, named “GGvis” and “XGvis”, that implement these techniques.

MDS is a method for visualizing proximity data, that is, data where objects are characterized by dissimilarity values for all pairs of objects. MDS constructs maps (called “configurations”) of these objects in  $\mathbb{R}^k$  by interpreting the dissimilarities as distances.

As a data-mapping technique, MDS is fundamentally a visualization method. It is hence plausible that MDS gains in power if it is embedded in a data visualization environment. Consequently, the MDS systems presented here are conceived as extensions of multivariate data visualization systems (“GGvis” and “X/GGobi” in this case). The visual analysis of MDS output profits from dynamic projection tools for viewing high-dimensional configurations, from brushing multiple linked views, from plot enhancements such as labels, glyphs, colors, lines, and from selective removal of groups of objects. Powerful is also the ability to move points and groups of points interactively and thereby create new starting configurations for MDS optimization.

In addition to the benefits of a data visualization environment, we enhance MDS by providing interactive control over numerous options and parameters, a few of them novel. They include choices of 1) metric versus nonmetric MDS, 2) classical versus distance MDS, 3) the configuration dimension, 4) power transformations for metric MDS, 5) distance transformations and 6) Minkowski metrics for distance MDS, 7) weights in

---

<sup>1</sup>Andreas Buja is the Liem Sioe Liong / First Pacific Company Professor, The Wharton School, University of Pennsylvania, Philadelphia, PA 19104-6302. (<http://www-stat.wharton.upenn.edu/~buja>)

<sup>2</sup>Deborah F. Swayne is Senior Technical Staff Member, AT&T Labs, 180 Park Ave., P.O. Box 971, Florham Park, NJ 07932-0971. ([dfs@research.att.com](mailto:dfs@research.att.com), <http://www.research.att.com/~dfs>)

<sup>3</sup>Michael L. Littman is Associate Research Professor, Rutgers University, Department of Computer Science, Hill Center Room 409, Piscataway, NJ 08854-8019. ([mlittman@cs.rutgers.edu](mailto:mlittman@cs.rutgers.edu), <http://www.cs.rutgers.edu/~mlittman/>)

<sup>4</sup>Nathaniel Dean is Associate Professor, Computational and Applied Mathematics - MS 134, Rice University, 6100 Main Street, Houston, TX 77005. ([nated@caam.rice.edu](mailto:nated@caam.rice.edu), <http://www.caam.rice.edu/~nated>)

<sup>5</sup>Heike Hofmann is Assistant Professor, Dept of Statistics, Iowa State University, Ames, IA 50011. ([heike@iastate.edu](mailto:heike@iastate.edu), <http://www1.math.uni-augsburg.de/~hofmann>)

the form of powers of dissimilarities and 8) as a function of group memberships, 9) various types of group-dependent MDS such as multidimensional unfolding and external unfolding, 10) random subselection of dissimilarities, 11) perturbation of configurations, and 12) a separate window for diagnostics, including the Shepard plot.

MDS was originally developed for the social sciences, but it is now also used for laying out graphs. Graph layout is usually done in 2-D, but we allow layouts in arbitrary dimensions. We show applications to the mapping of computer usage data, to the dimension reduction of marketing segmentation data, to the layout of mathematical graphs and social networks, and finally to the spatial reconstruction of molecules.

**Key Words:** Proximity Data, Dissimilarity Data, Multivariate Analysis, Dimension Reduction, Multidimensional Unfolding, External Unfolding, Graph Layout, Social Networks, Molecular Conformation.

# 1 Introduction: Basics of Multidimensional Scaling

This paper is about functionality that proves useful for the application and interpretation of MDS. In a companion paper (Buja and Swayne 2002) we describe methodology that is supported by the functionality.

The present section gives a short introduction to those types of MDS that are relevant for this article. Section 2 gives an overview of how a user operates the XGvis or GGvis system. Section 3 deals with algorithm animation, direct manipulation and perturbation of the configuration. Section 4 gives details about the cost functions and their interactively controlled parameters for transformation, subsetting and weighting of dissimilarities. Section 5 describes diagnostics for MDS. Section 6 is about computational and systems aspects, including coordination of windows, algorithms, and large data problems. Finally, Section 7 gives a tour of applications with examples of proximity analysis, dimension reduction, and graph layout in two and more dimensions.

**Software availability:** The XGvis and GGvis systems can be freely downloaded, respectively, from:

[www.research.att.com/areas/stat/xgobi/](http://www.research.att.com/areas/stat/xgobi/)  
[www.ggobi.org](http://www.ggobi.org)

XGvis is currently more established, but GGvis is more recent, easier to run under MS Windows, and programmable from other systems such as R. In what follows we refer to the two systems as X/GGvis.

## 1.1 Proximity Data and Stress Functions

Multidimensional scaling (MDS) is a family of methods for analyzing proximity data. Proximity data consist of similarity or, equivalently, dissimilarity information for *pairs of objects*.

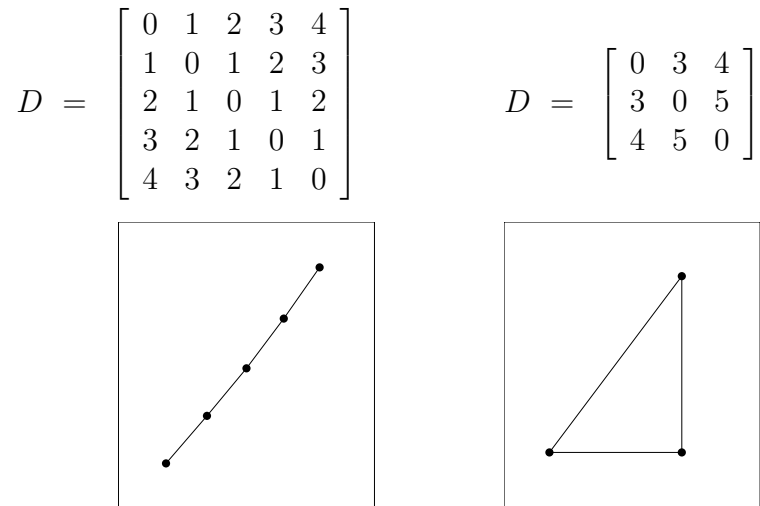


Figure 1: *Simple Examples of Dissimilarity Matrices and Their Optimal Scaling Solutions.*

This contrasts with multivariate data that consist of covariate information for *individual objects*. If the objects are labeled  $i = 1, \dots, N$ , proximity data can be assumed to be dissimilarity values  $D_{i,j}$ . If the data are given as similarities, some monotone decreasing transformation will convert them to dissimilarities. Dissimilarity data occur in many areas (see Section 1.3).

The goal of MDS is to map the objects  $i = 1, \dots, N$  to points  $\mathbf{x}_1, \dots, \mathbf{x}_N \in \mathbb{R}^k$  in such a way that the given dissimilarities  $D_{i,j}$  are well-approximated by the distances  $\|\mathbf{x}_i - \mathbf{x}_j\|$ . Psychometricians often call these distances the “model” fitted to the data  $D_{i,j}$ .

The dissimilarity matrices of Figure 1 are simple examples with easily recognized error-free MDS solutions: the left matrix suggests mapping the five objects to an equispaced linear arrangement; the right matrix suggests mapping the three objects to a right triangle. The figure shows configurations actually found by MDS. The first configuration can be embedded in  $k = 1$  dimension, while the second needs  $k = 2$  dimensions. The choice of embedding dimension  $k$  is arbitrary in principle, but low in practice:  $k = 1, 2, 3$  are the most frequently used dimensions, for the simple reason that the points serve as easily visualized representors of the objects.

In real data, there are typically many more objects, and the dissimilarities usually contain error as well as bias with regard to the fitted distances.

The oldest version of MDS, called classical scaling, is due to Torgerson (1952). It is, however, a later version due to Kruskal (1964a,b) that has become the leading MDS method. It is defined in terms of minimization of a cost function called “Stress”, which is simply a measure of lack of fit between dissimilarities  $D_{i,j}$  and distances  $\|\mathbf{x}_i - \mathbf{x}_j\|$ . In the simplest case, Stress is a residual sum of squares:

$$\text{Stress}_D(\mathbf{x}_1, \dots, \mathbf{x}_N) = \left( \sum_{i \neq j=1..N} (D_{i,j} - \|\mathbf{x}_i - \mathbf{x}_j\|)^2 \right)^{1/2} \quad (1)$$

where the outer square root is just a convenience that gives greater spread to small values. For a given dissimilarity matrix  $D = (D_{i,j})$ , MDS minimizes Stress over all point configurations  $(\mathbf{x}_1, \dots, \mathbf{x}_N)$ , thought of as  $k \times N$ -dimensional hypervectors of unknown parameters. The minimization can be carried out by straightforward gradient descent applied to  $\text{Stress}_D$ , viewed as a function on  $\mathbb{R}^{kN}$ .

We note a technical detail: MDS is blind to asymmetries in the dissimilarity data because

$$(D_{i,j} - \|\mathbf{x}_i - \mathbf{x}_j\|)^2 + (D_{j,i} - \|\mathbf{x}_j - \mathbf{x}_i\|)^2 = 2 \cdot ((D_{i,j} + D_{j,i})/2 - \|\mathbf{x}_i - \mathbf{x}_j\|)^2 + \dots,$$

where  $\dots$  is an expression that does not depend on  $\|\mathbf{x}_i - \mathbf{x}_j\|$ . Without loss of generality we assume from now on that the dissimilarities are symmetric:  $D_{i,j} = D_{j,i}$ . If they are not, they should be symmetrized by forming pairwise averages. The assumption of symmetry will later be broken in one special case, when one of the two values is permitted to be missing (Section 4.4).

## 1.2 Types of Multidimensional Scaling

There exist many MDS methods, differing mostly in the cost function they use. Here are two dichotomies that allow us to structure some possibilities:

- **Kruskal-Shepard distance scaling** versus **classical Torgerson-Gower inner-product scaling**: Distance scaling is based on direct fitting of distances to dissimilarities, whereas the older classical scaling is based on a detour whereby dissimilarities are converted to a form that is naturally fitted by inner products  $\langle \mathbf{x}_i, \mathbf{x}_j \rangle$  (see below).
- **Metric scaling** versus **nonmetric scaling**: Metric scaling uses the actual values of the dissimilarities, while nonmetric scaling effectively uses only their ranks (Shepard 1962, Kruskal 1964a). Nonmetric MDS is realized by estimating an optimal monotone transformation  $f(D_{i,j})$  of the proximities simultaneously with the configuration.

In X/GGvis we implemented both distance scaling and classical inner-product scaling, and both metric and nonmetric scaling. In all, four types of MDS are provided: metric distance, nonmetric distance, metric classical, and nonmetric classical scaling. The unusual case of nonmetric classical scaling will be described in Section 4.2.

A *conceptual difference* between classical and distance scaling is that inner products rely on an origin, while distances do not; a set of inner products determines uniquely a set of distances, but a set of distances determines a set of inner products only modulo change of origin. To avoid arbitrariness, one constrains classical scaling to configurations with the mean at the origin.

The *computational difference* between classical and distance scaling is that the minimization problem for classical scaling can be solved with a simple eigendecomposition, while distance scaling requires iterative minimization. In X/GGvis, though, classical scaling is implemented with iterative gradient descent of a cost function called “Strain”, as is distance scaling with regard to Stress. This computational uniformity has advantages: it is straightforward to introduce weights and missing values in Strain and Stress, but not so in eigendecompositions. Both weights and missing values are extensively used in X/GGvis.

### 1.3 Applications of MDS

Here is an incomplete list of application areas for MDS:

- MDS was invented for the *analysis of proximity data* which arise in the following areas:
  - *The social sciences*: Proximity data take the form of similarity ratings for pairs of stimuli such as tastes, colors, sounds, people, nations, ...
  - *Archaeology*: Similarity of two digging sites can be quantified based on the frequency of shared features in artifacts found in the sites.
  - *Classification problems*: In classification with large numbers of classes, pairwise misclassification rates produce confusion matrices that can be analyzed as similarity data. An example would be confusion rates of phonemes in speech recognition.
- Another early use of MDS was for *dimension reduction*: Given high-dimensional data  $\mathbf{y}_1, \dots, \mathbf{y}_N \in \mathbb{R}^K$  ( $K$  large), compute a matrix of pairwise distances  $\text{dist}(\mathbf{y}_i, \mathbf{y}_j) = D_{i,j}$ , and use distance scaling to find lower-dimensional  $\mathbf{x}_1, \dots, \mathbf{x}_N \in \mathbb{R}^k$  ( $k \ll K$ ) whose pairwise distances reflect the high-dimensional distances  $D_{i,j}$  as well as possible. In this application, distance scaling is a non-linear competitor of principal components. Classical scaling, on the other hand, is identical to principal components when used for dimension reduction. For a development of multivariate analysis from the point of view of distance approximation, see Meulman (1992).
- In chemistry, MDS can be used for *molecular conformation*, that is, the problem of reconstructing spatial structure of molecules. This situation differs from the above areas in that 1) actual distance information is available from experiments or theory, and 2) the only meaningful embedding dimension is  $k = 3$ , physical space. Configurations are here called “conformations.” Some references are Crippen and Havel (1978), Havel (1991), Glunt et al. (1993), and Trosset (1998a). See also our nanotube example in Section 7.
- A fourth use of MDS is for *graph layout*, an active area at the intersection of discrete mathematics and network visualization, see Di Battista et al. (1994). An early example before its time was Kruskal and Seery (1980). From graphs one can derive distances, such as shortest-path metrics, which can be subjected to MDS for planar or spatial layout. Note that shortest-path metrics are generally strongly non-Euclidean, hence significant residual should be expected in this type of application.

In Section 7 we will show examples of data in all four categories. Our overall experience with the various types of MDS is as follows: distance scaling is sometimes not very good at dimension reduction, whereas classical inner-product scaling is sometimes not very good at graph layout. The examples will exemplify these points.

### 1.4 A First Example: The Rothkopf Morse Code Data

For illustration we use as our running example the well-known Rothkopf Morse code data (1957) (available with the X/GGvis distributions). They are to MDS what Fisher’s Iris data

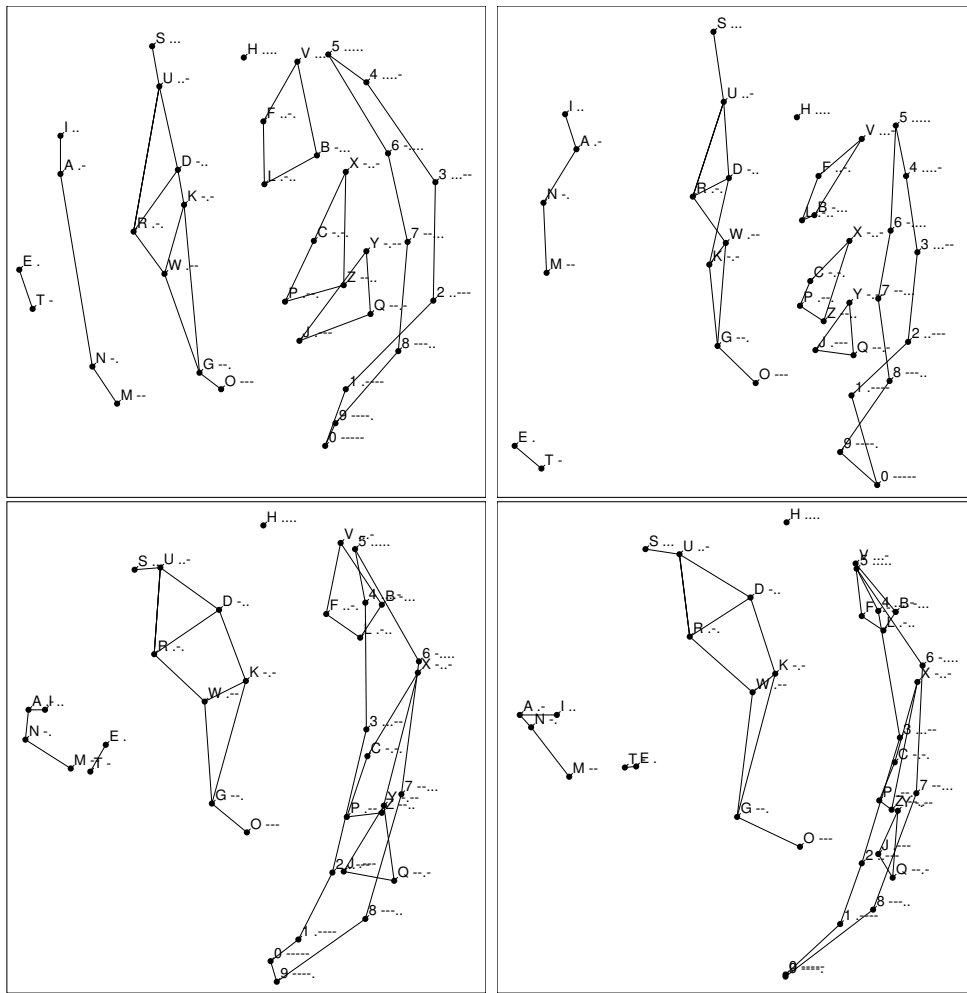


Figure 2: *Rothkopf's Morse Code Data: four 2-D configurations. Top row: metric and nonmetric distance scaling. Bottom row: metric and nonmetric classical scaling.*

are to discriminant analysis. They originated in an experiment where inexperienced subjects were exposed to pairs of Morse codes in rapid order. The subjects had to decide whether the two codes in a pair were identical or not. The data were summarized in a table of confusion rates.

Confusion rates are similarity measures: codes that are often confused are interpreted as “similar” or “close.” Similarities need to be converted to dissimilarities. Any monotone decreasing transformation can be used for conversion, but we used the following:

$$D_{i,j}^2 = s_{i,i} + s_{j,j} - 2s_{i,j} .$$

This yielded all non-negative values because the confusion matrix  $(s_{i,j})_{i,j}$  is diagonally dominant (most identical code pairs are correctly judged even by inexperienced subjects). Unlike other conversion methods, this one has the desirable property  $D_{i,i} = 0$ . We also sym-

metrized the dissimilarities before the conversion as MDS responds only to the symmetric part of proximity data, as noted earlier.

Applying all four scaling methods in  $k = 2$  dimensions to the Morse code dissimilarities produced the configurations shown in Figure 2. We decorated the plots with labels and lines to aid interpretation. In particular, we connected groups of codes of the same length, except for codes of length four which we broke up into three groups and a singleton. We observe that, roughly, the length of the codes increases left to right, and the fraction of dots increases bottom up. Both of these observations agree with the many published accounts (Shepard 1962, Kruskal and Wish 1978, p. 13, Borg and Groenen 1997, p. 59, for example). The orientation of the configurations in  $\mathbb{R}^2$  is arbitrary due to rotation invariance of the distances  $\|\mathbf{x}_i - \mathbf{x}_j\|$  and inner products  $\langle \mathbf{x}_i, \mathbf{x}_j \rangle$ . We were therefore free to rotate the configurations in order to achieve this particular interpretation of the horizontal and vertical axes.

The configurations produced by the four scaling methods show significant differences. Nonmetric distance scaling (top right) produces probably the most satisfying configuration, with the exception of the placement of the codes of length 1 (“E” and “T”). Metric scaling (top left) suffers from circular bending but it places “E” and “T” in the most plausible location. The classical scaling methods (bottom row) bend the configurations in different ways. More problematically, they overlay the codes of length 4 and 5 and invert the placement of the codes of length 1 and 2, both of which seem artifactual. In fact they aren’t: classical scaling requires a third dimension to distinguish between these two pairs of groups. Distance scaling is better at achieving compromises in lower dimensions, while classical scaling is more rigid in this regard.

## 2 Interactive MDS Operation

The main use of MDS configurations is for visualization. Because configurations are essentially multivariate data, any MDS system calls for a multivariate data visualization tool. Two of us being co-authors of the XGobi and GGobi systems for data visualization, it was natural that we chose them as viewing engines (XGobi: Swayne, Cook and Buja 1998, Buja, Cook and Swayne 1996; GGobi: Swayne, Buja and Temple Lang 2003, Swayne, Temple Lang, Buja and Cook 2002). We thus conceived of X/GGvis as master programs that create and feed X/GGobi windows. Figure 3 shows how this presents itself to the user in the case of GGobi: a master panel with MDS controls (left), a GGobi window for viewing the configuration (right), and a discretionary GGobi window for diagnostics (bottom).

In what follows, we make X/GGvis and X/GGobi operations recognizable by placing them in quotation marks. The basic sequence of MDS interactions is as follows:

- Start up with dissimilarity data, multivariate data, or graph data. X/GGvis will perform proximity analysis, dimension reduction, or graph layout, respectively. Provide an initial configuration, or else a random configuration is generated automatically.
- Select one of the four scaling methods. The default is metric distance scaling.
- Choose a dimension. The default is 3.

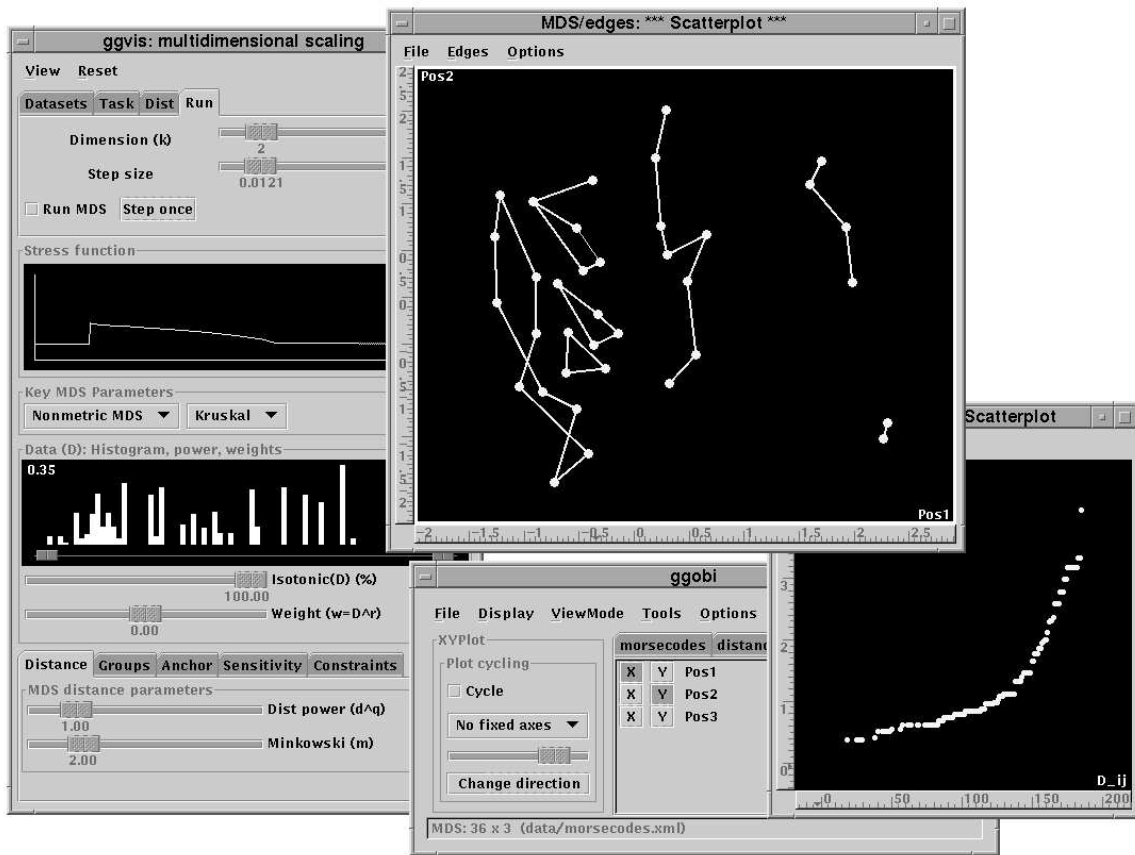


Figure 3: *The Major GGvis Windows. On the left is the master control panel, on the right is the GGobi window for the configuration. Below is the GGobi window for an optional Shepard plot.*

- Initiate optimization (“Run MDS”) and watch the animation of the configuration and the progression of the Stress or Strain value. When the shape of the configuration stops changing, slow the optimization down by lowering the stepsize interactively. Finally, stop the optimization (toggle “Run MDS”). X/GGvis does not have an automatic convergence criterion, and optimization does not stop on its own.
- Examine the shape of the optimized configuration: If the chosen dimension  $k$  is two, remain in “XY Plot”. If  $k$  is three, use 3-D “Rotation” or the “Grand/2-D Tour”. If  $k$  is higher, use the “Grand/2-D Tour”.
- Interpret the configuration: Assuming informative object labels were provided with the input data, search the configuration by labeling points (“Identify”). If covariates are available in addition to the dissimilarities, interpretation can be further aided by linked color brushing between covariate views and configuration views (“Brush”). Multiple X/GGobi windows are automatically linked for brushing and labeling. As this is only a tentative search for interpretable structure, use “transient” brushing.

- Enhance the configuration: After acquiring a degree of familiarity with the configuration, use “persistent” brushing in order to permanently characterize subsets of interest. Enhance the configuration further by persistently labeling interesting points. Finally, enhance the overall perception of shape by connecting selected pairs of nearby points with lines (“Line Editing”) and coloring the lines (“Brush”).
- Turn on optimization and leave it continually running. Observe the effects of
  - experimenting with various parameters,
  - subsetting objects,
  - subsetting dissimilarities,
  - weighting dissimilarities,
  - manually moving points and groups of points.
  - perturbing the configuration or restarting from random configurations.
- Stop optimization and perform diagnostics by generating a separate X/GGobi window that shows among other things a “Shepard plot” of the transformed dissimilarities and the fitted distances.

We described elsewhere (Swayne et al. 1998) X/GGobi operations such as three-D rotations and grand tours, as well as (linked) brushing, labeling and line editing. Moving points is also an X/GGobi operation, but in conjunction with MDS optimization it takes on a special importance and is therefore described in Section 3. MDS parameters as well as weighting and subsetting of dissimilarities affect the cost function and are therefore specific to MDS. They are the subject of Section 4.

### 3 Animated Optimization and Point Manipulation

At the time of writing, most software for MDS still works with batch processing, even though many older programs have been wrapped in somewhat interactive PC environments. A pioneering system that is truly interactive in our meaning of the term is McFarlane and Young’s “ViSta-MDS” (1994). Development of this system took place around the time when we developed a first version of XGvis (Littman et al. 1992). Although the two systems were developed independently, they share two important interactive capabilities:

1. **Animated Optimization:** The configuration points are displayed continuously as they are subjected to MDS optimization. For a series of stills from an animated optimization, see Figure 4. At the same time, the values of the cost function are also shown in a trace plot (Figure 3).
2. **Manual Dragging:** Configuration points can be moved interactively with mouse dragging.

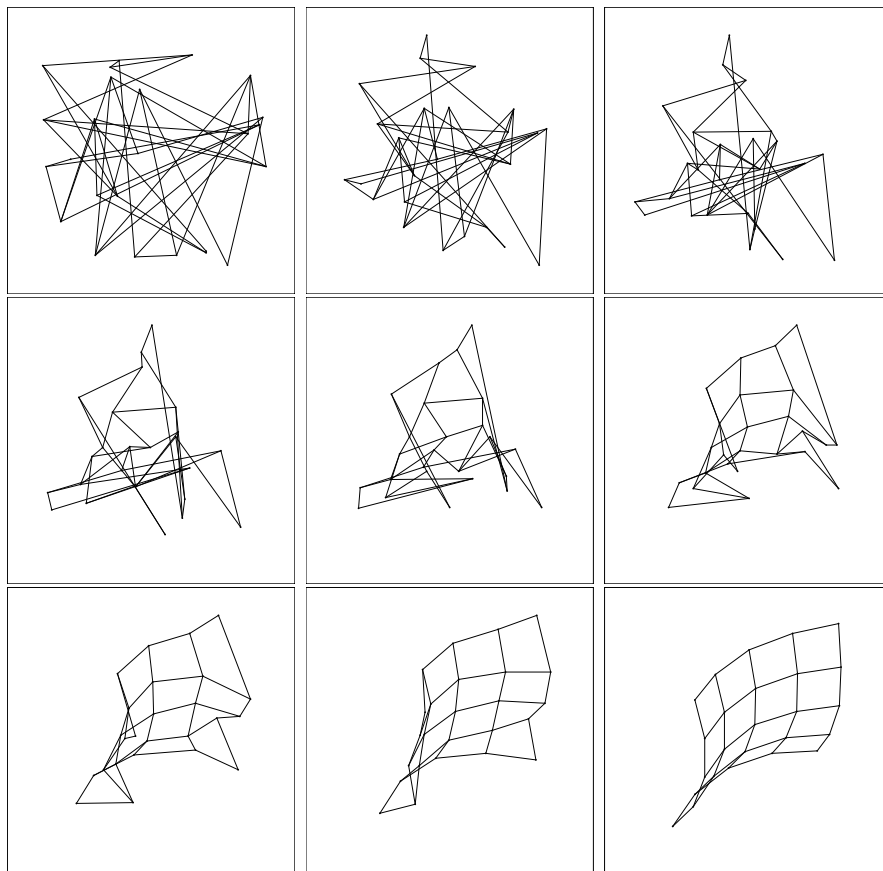


Figure 4: *Snapshots from a MDS Animation.* The figure shows nine stages of a Stress minimization in three dimensions. It reconstructed a  $5 \times 5$  square grid from a random configuration. The grid was defined as a graph with 25 nodes and 40 edges. The distances were computed as the lengths of the minimal paths in the graph (= city block-, Manhattan-, or  $L_1$ -distances). These distances are not Euclidean, causing curvature in the configuration.

McFarlane and Young call this methodology “sensitivity analysis” because moving points and observing the response of the optimization amounts to checking the stability of the configuration.

ViSta-MDS implements a *two-step mode of operation* in which users alternate between animated optimization and manipulation. X/GGvis permits the two-step mode also, but in addition it implements a *fluid mode of operation* in which the user runs a never-ending optimization loop, with no stopping criterion whatsoever. The user manipulates the configuration points while the optimization is in progress. The optimizer ignores the manipulated point, but the other points “feel” the dislocation through the change in the cost function, and they are therefore slowly dragged. They try to position themselves in a local minimum configuration with regard to the manipulated point. As soon as the manipulated point is let go, it snaps into a position that turns the configuration into a local minimum of the cost function. The resulting feel for the user is that of pricking and tearing the fabric of the

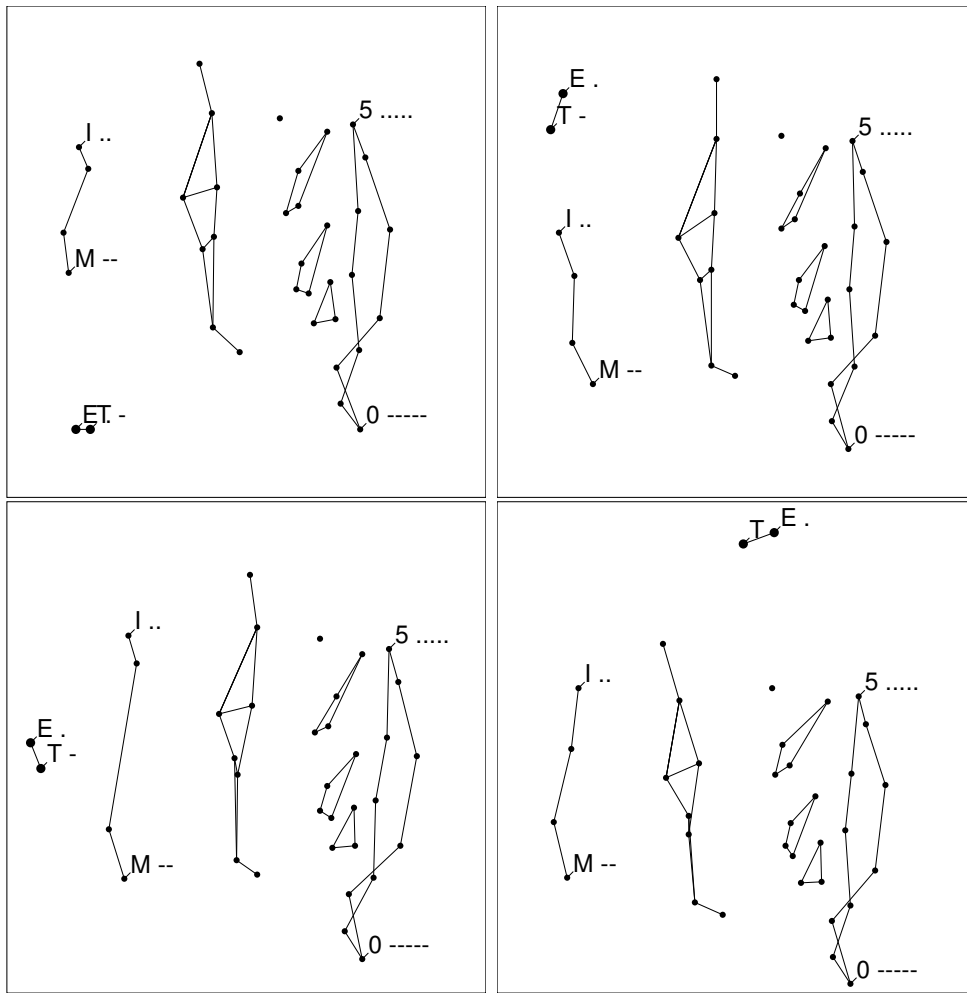


Figure 5: *Four Local Minima Found by Moving the Group  $\{E, T\}$  into Different Locations. The Stress values are, left to right and top to bottom: 0.2101, 0.2187, 0.2189, 0.2207.*

configuration while exploring deformations of its shape.

In addition to moving one point at a time, X/GGvis permits *moving groups of points* defined by shared point glyphs and colors. This capability can be helpful when it has become evident that certain points always stay together, as in the Morse code data the points for the codes of length one (“E” and “T”). The only way to find further local minima is by moving the points jointly. Indeed, when the Morse code data are mapped into two dimensions with metric distance scaling and a third power transformation (which mimics a nonmetric solution very well), we found four different locally optimal locations for the codes of length one (Figure 5). Another two local minimum configurations can be found by moving the codes of length two.

More local minima can be found by restarting optimization with a *random configuration* (X/GGvis provides Gaussian random point clouds). In addition, it is possible to examine local stability by *perturbing a configuration* with normal random numbers by forming a con-

vex mixture of the present configuration and a random Gaussian configuration. The default mixing parameter is 100% random, which means a completely new random configuration is generated. A smaller fraction of 20% or so can be used for local stability checks: if optimization always drives the perturbed configuration back to its previous state, it is stable under 20% perturbation. Further stability checks will be discussed below. For a discussion of the problem of local minimum configurations, see Borg and Groenen (1997), Section 13.4.

As a final point, here is another use of manual dragging: *rotation of configurations* for interpretability, essentially the factor rotation problem translated to MDS. After examining a configuration and decorating it with labels, colors, glyphs and lines, one usually obtains interpretations of certain directions in configuration space. This is when one develops a desire to rotate the configuration to line these directions up with the horizontal and vertical axes. One can achieve this by dragging points while optimization is running continuously. When points are moved gently, the optimization will try to rotate the configuration so that the moved point maintains a local minimum location relative to the other points. We used this effect to rotate the four configurations of Figure 2 into their present orientations.

## 4 Cost Functions: Stress and Strain

As mentioned in the introduction, we use iterative minimization of cost functions even where eigendecompositions would work, the reason being that missing and weighted dissimilarities are handled with difficulty by the latter but trivially by the former. We develop the specific forms of Stress and Strain used in X/GGvis.

### 4.1 Stress

Although the simplest form of cost function for distance scaling is a residual sum of squares, it is customary to report Stress values that are standardized and unit-free. This may take the form

$$\text{Stress}_D(\mathbf{x}_1, \dots, \mathbf{x}_N) = \left( \frac{\sum_{i,j} (D_{i,j} - \|\mathbf{x}_i - \mathbf{x}_j\|)^2}{\sum_{i,j} D_{i,j}^2} \right)^{1/2}$$

In this form of Stress one can explicitly optimize the size of the configuration:

$$\min_t \text{Stress}_D(t \cdot \mathbf{x}_1, \dots, t \cdot \mathbf{x}_N) = \left( 1 - \frac{(\sum_{i,j} D_{i,j} \cdot \|\mathbf{x}_i - \mathbf{x}_j\|)^2}{\sum_{i,j} D_{i,j}^2 \cdot \sum_{i,j} \|\mathbf{x}_i - \mathbf{x}_j\|^2} \right)^{1/2}$$

This ratio inside the parens can be interpreted geometrically as the squared cosine between the “vectors”  $\{D_{i,j}\}_{i,j}$  and  $\{\|\mathbf{x}_i - \mathbf{x}_j\|\}_{i,j}$ , which is hence a number between zero and one. The complete right hand side is therefore the sine between these two vectors. This is the form of Stress reported and traced by X/GGvis.

The Stress we actually use is of considerably greater generality, however: it permits 1) power transformations of the dissimilarities in metric mode and isotonic transformations

in nonmetric mode, 2) Minkowski distances in configuration space, 3) powers of the distances, 4) weighting of the dissimilarities, and 5) missing and omitted dissimilarities. We give the complete formula for Stress as implemented and defer the explanation of details to Section 4.3:

$$\text{STRESS}_D(\mathbf{x}_1, \dots, \mathbf{x}_N) = (1 - \cos^2)^{1/2}$$

$$\cos^2 = \frac{\left( \sum_{(i,j) \in I} w_{i,j} \cdot f(D_{i,j}) \cdot \|\mathbf{x}_i - \mathbf{x}_j\|_m^q \right)^2}{\left( \sum_{(i,j) \in I} w_{i,j} \cdot f(D_{i,j})^2 \right) \left( \sum_{(i,j) \in I} w_{i,j} \cdot \|\mathbf{x}_i - \mathbf{x}_j\|_m^{2q} \right)}$$

$D_{i,j} \in \mathbb{R}, \geq 0$ ,  $N \times N$  matrix of dissimilarity data

$$f(D_{i,j}) = \begin{cases} D_{i,j}^p, & \text{for metric MDS} \\ s \cdot \text{Isotonic}(D_{i,j}) + (1 - s) \cdot D_{i,j}^p, & \text{for nonmetric MDS} \end{cases}$$

$0 \leq p \leq 6$ , default:  $p = 1$  (no transformation)  
 $0 \leq s \leq 1$ , default:  $s = 1$  (fully isotonic transformation)  
 Isotonic = monotone  $\uparrow$  transformation estimated  
 with isotonic regression

$\mathbf{x}_1, \dots, \mathbf{x}_N \in \mathbb{R}^k$ , configuration points;  $1 \leq k \leq 12$ , default:  $k = 3$

$$\|\mathbf{x}_i - \mathbf{x}_j\|_m^q = \left( \sum_{\nu=1, \dots, k} |x_{i,\nu} - x_{j,\nu}|^m \right)^{q/m}, \quad \text{configuration distances, } (.)^q$$

$1 \leq m \leq 6$ ,  $m = 2$ : Euclidean (default)  
 $m = 1$ : City block  
 $0 \leq q \leq 6$ ,  $q = 1$ : common Stress (default)  
 $q = 2$ : so-called SStress

The summation set  $I$  and the weights  $w_{i,j}$  will be discussed in Section 4.5.

## 4.2 Strain, Metric and Nonmetric

Classical scaling is based on inner products, which unlike distances depend on the origin. One standardizes the procedure by assuming configurations with zero mean:  $\sum_i \mathbf{x}_i = 0$ . Under this assumption, one fits inner products  $\langle \mathbf{x}_i, \mathbf{x}_j \rangle$  to a transformation of the dissimilarity data. The derivation of this transformation is based on the following heuristic:

$$D_{i,j}^2 \approx \|\mathbf{x}_i - \mathbf{x}_j\|^2 = \|\mathbf{x}_i\|^2 + \|\mathbf{x}_j\|^2 - 2\langle \mathbf{x}_i, \mathbf{x}_j \rangle$$

As the matrix  $(\langle \mathbf{x}_i, \mathbf{x}_j \rangle)_{i,j}$  has zero row and column means, one recognizes that the necessary transformation is simply the removal of row and column means from the matrix

$$\tilde{D}_{i,j} := -D_{ij}^2/2,$$

a process which is commonly known as “double-centering”:

$$B_{ij} = \tilde{D}_{ij} - \tilde{D}_{i\bullet} - \tilde{D}_{\bullet j} + \tilde{D}_{\bullet\bullet} ,$$

where  $\tilde{D}_{i\bullet}$ ,  $\tilde{D}_{\bullet j}$  and  $\tilde{D}_{\bullet\bullet}$  are row, column and grand means. The quantities  $B_{i,j}$  are now plausibly called “inner-product data”:

$$B_{i,j} \approx \langle \mathbf{x}_i, \mathbf{x}_j \rangle$$

We call “Strain” any cost function that involves inner products of configuration points and inner-product data. One form of Strain is a standardized residual sum of squares between the quantities  $B_{i,j}$  and the inner products:

$$\text{Strain}_D(\mathbf{x}_1, \dots, \mathbf{x}_N) = \left( \frac{\sum_{i,j} (B_{i,j} - \langle \mathbf{x}_i, \mathbf{x}_j \rangle)^2}{\sum_{i,j} \langle \mathbf{x}_i, \mathbf{x}_j \rangle^2} \right)^{1/2}$$

In size-minimized form this is:

$$\min_t \text{Strain}_D(t \cdot \mathbf{x}_1, \dots, t \cdot \mathbf{x}_N) = \left( 1 - \frac{(\sum_{i,j} B_{i,j} \cdot \langle \mathbf{x}_i, \mathbf{x}_j \rangle)^2}{\sum_{i,j} B_{i,j}^2 \cdot \sum_{i,j} \langle \mathbf{x}_i, \mathbf{x}_j \rangle^2} \right)^{1/2}$$

Again, this is not the form of Strain we use. Instead, we pose ourselves the problem of finding a form that can be made nonmetric. Nonmetric classical MDS seems a contradiction in terms because classical scaling must be metric according to the conventional interpretations. Yet we may ask whether it would not be possible to transform the dissimilarity data  $D_{i,j}$  in such a way that a better Strain could be obtained, just as the data are transformed in nonmetric distance scaling to obtain a better Stress. This is indeed possible, and a solution has been given by Trosset (1998b). We give here an alternative derivation with additional simplifications that permit us to fit the Strain minimization problem in the existing framework. Classical nonmetric scaling is not a great practical advance, but it fills a conceptual gap. It also gives the software a more satisfactory structure by permitting all possible pairings of {metric, nonmetric} with {classical scaling, distance scaling}. The properties of nonmetric classical scaling are not well-understood at this point. The implementation in X/GGvis will hopefully remedy the situation.

We start with the following observations:

- Because the matrix  $(B_{i,j})_{i,j}$  is doubly-centered, any Strain-minimizing configuration is centered at the origin.
- If, however, the configuration is constrained to be centered at the origin, one may use  $(-D_{i,j}^2/2)_{i,j}$  instead of  $(B_{i,j})_{i,j}$  in the Strain formula; the minimizing configurations will be the same. That is, double centering of  $(-D_{i,j}^2/2)_{i,j}$  may be replaced with forced centering of the configuration.

The first bullet is almost tautological in view of our introduction of classical scaling. The second bullet may be new; it is certainly the critical one. To elaborate we need a little linear algebra:

If  $A$  and  $C$  are  $N \times N$  matrices, denote by  $\langle A, C \rangle_F = \text{trace}(A^T C) = \sum_{i,j} A_{i,j} C_{i,j}$  the Frobenius inner product, and by  $\|A\|_F = \langle A, A \rangle_F^{1/2}$  the Frobenius norm. Furthermore, let  $\mathbf{e} = (1, \dots, 1)^T \in \mathbb{R}^N$  and  $I_N$  be the  $N \times N$  identity matrix, so that  $P = I_N - \mathbf{e}\mathbf{e}^T/N^{1/2}$  is the centering projection. Then the equation  $B_{i,j} = \tilde{D}_{i,j} - \tilde{D}_{i\bullet} - \tilde{D}_{\bullet j} + \tilde{D}_{\bullet\bullet}$  can be re-expressed as  $B = P\tilde{D}P$ . Finally, let  $X$  be the  $N \times k$  configuration matrix whose rows contain the coordinates of the configuration points, so that  $(\langle \mathbf{x}_i, \mathbf{x}_j \rangle)_{i,j} = XX^T$ . The centering condition  $\sum_i \mathbf{x}_i = 0$  can be re-expressed as  $PX = X$ , and the residual sum of squares of Strain as

$$\sum_{i,j} (B_{i,j} - \langle \mathbf{x}_i, \mathbf{x}_j \rangle)^2 = \|B - XX^T\|_F^2.$$

Using repeatedly a basic property of traces,  $\text{trace}(A^T C) = \text{trace}(C^T A)$ , one derives  $\langle B, XX^T \rangle_F = \langle B, PXX^T P \rangle_F$  and hence:

$$\|B - XX^T\|_F^2 = \|B - PXX^T P\|_F^2 + \|PXX^T P - XX^T\|_F^2.$$

Therefore, a minimizing configuration matrix satisfies  $PX = X$ , which shows the first bullet above. For the second bullet, assume  $PX = X$  and observe that  $\langle \tilde{D}, XX^T \rangle_F = \langle P\tilde{D}P, XX^T \rangle_F = \langle B, XX^T \rangle_F$ . It follows

$$\|\tilde{D} - XX^T\|_F^2 = \|\tilde{D} - B\|_F^2 + \|B - XX^T\|_F^2.$$

Therefore, under the constraint  $\sum_i \mathbf{x}_i = 0$  minimizing  $\sum_{i,j} ((-D_{i,j}^2/2) - \langle \mathbf{x}_i, \mathbf{x}_j \rangle)^2$  is the same as minimizing  $\sum_{i,j} (B_{i,j} - \langle \mathbf{x}_i, \mathbf{x}_j \rangle)^2$  as the two cost functions differ only by a constant.

The former cost function has the property we were looking for: it lends itself to a non-metric extension by replacing the original transformation  $-D_{i,j}^2/2$  with a general descending transformation  $f(-D_{i,j})$ , where  $f$  is a monotone increasing (non-decreasing) function that can be estimated with isotonic regression of  $\langle \mathbf{x}_i, \mathbf{x}_j \rangle$  on  $-D_{i,j}$ . In the metric case, an extension to power transformations is natural:  $f(-D_{i,j}) = -D_{i,j}^{2p}$ . Thus we have solved the problem of finding a natural nonmetric form of classical scaling.

Like Stress, the Strain actually implemented in X/GGvis is a standardized size-optimized version (to avoid the collapse of  $f(-D_{i,j})$ ), and it also has some generalizations such as weighting and omitting of dissimilarities:

$$\begin{aligned} \text{STRAIN}_D(\mathbf{x}_1, \dots, \mathbf{x}_N) &= (1 - \cos^2)^{1/2} \\ \cos^2 &= \frac{\left( \sum_{(i,j) \in I} w_{i,j} \cdot f(-D_{i,j}) \cdot \langle \mathbf{x}_i, \mathbf{x}_j \rangle \right)^2}{\left( \sum_{(i,j) \in I} w_{i,j} \cdot f(-D_{i,j})^2 \right) \left( \sum_{(i,j) \in I} w_{i,j} \cdot \langle \mathbf{x}_i, \mathbf{x}_j \rangle^2 \right)} \end{aligned}$$

$D_{i,j} \in \mathbb{R}, \geq 0$ ,  $N \times N$  matrix of dissimilarity data

$$f(-D_{i,j}) = \begin{cases} -D_{i,j}^{2p}, & \text{for metric MDS} \\ s \cdot \text{Isotonic}(-D_{i,j}) + (1-s) \cdot (-D_{i,j}^{2p}), & \text{for nonmetric MDS} \end{cases}$$

$0 \leq p \leq 6$ , default:  $p = 1$  (no transformation)  
 $0 \leq s \leq 1$ , default:  $s = 1$  (fully isotonic transformation)  
 Isotonic = monotone  $\uparrow$  transformation estimated  
 with isotonic regression

$\mathbf{x}_1, \dots, \mathbf{x}_N \in \mathbb{R}^k$ , configuration points, constrained to  $\sum \mathbf{x}_i = 0$   
 $1 \leq k \leq 12$ , default:  $k = 3$

$$\langle \mathbf{x}_i, \mathbf{x}_j \rangle = \sum_{\nu=1, \dots, k} x_{i,\nu} \cdot x_{j,\nu}, \quad \text{configuration inner products}$$

The summation set  $I$  and the weights  $w_{i,j}$  will be discussed in Section 4.5.

### 4.3 Parameters of Stress and Strain

Stress and Strain have parameters that should be under interactive user control, as they are in X/GGvis:

- The most fundamental “parameters” are the discrete choices of metric versus nonmetric and distance versus classical scaling. The default is metric distance scaling.
- Next in importance is the choice of the dimension,  $k$ . The conventional choice is  $k = 2$ , but with 3-D rotations available it is plausible to chose  $k = 3$  as the default. For  $k \geq 4$  one can use the so-called “grand tour” or “2-Dtour”, a generalization of 3-D rotations to higher dimensions.
- Both metric and nonmetric scaling are controlled by a parameter that affects the transformation of the dissimilarities. The two parameters are very different in nature:
  - *Metric scaling* uses a *power transformation* with exponent  $p$ . The value  $p = 1$  (default) corresponds to no transformation. In our experience powers as high as 4 have proven useful. An interesting power is 0: in distance scaling it describes objects that form a simplex, that is, every object is equally far from every other object. This is the “null case” of total indiscrimination.
  - *Nonmetric scaling* is implemented in X/GGvis with a parameter  $s$  for *mixing of the isotonic transformation  $f(D_{i,j})$  with the metric power transform  $D_{i,j}^p$* . The value  $s = 1$  (default) corresponds to the isotonic transformation (purely nonmetric scaling), and  $s = 0$  to the pure power transformation (purely metric scaling). Sliding  $s$  across the interval  $[0, 1]$  while the MDS optimization is running shows transitions between a nonmetric and a metric solution. Moving  $s$  temporarily

below 1 can help a configuration recover when it gets trapped in a degeneracy (usually clumping of the points in a few locations, and near-zero Stress, see Borg and Groenen (1997) Sections 13.2-3). (In X/GGvis the power exponent  $p$  cannot be changed in nonmetric mode; it is inherited from the last visit to metric mode.)

- A parameter specific to distance scaling, both metric and nonmetric, is the distance power  $q$ . We introduced this parameter to include so-called SStress, which is obtained for  $p = q = 2$ . That is, SStress fits squared distances to squared dissimilarities. SStress is used in the influential MDS software “ALSCAL” by Takane et al. In our limited experience SStress is somewhat less robust than Stress, as the former is even more strongly influenced by large dissimilarities than Stress.
- There is finally a choice of metric in configuration space for distance scaling. We allow Minkowski (also called Lebesgue) metrics other than Euclidean by permitting the Minkowski parameter  $m$  to be manipulated. The default is Euclidean,  $m = 2$ ; the city block or  $L_1$  metric is the limiting case  $m \rightarrow 1$ .

## 4.4 Subsetting

The cost functions can trivially handle missing values in the dissimilarity matrix: Missing pairs  $(i, j)$  are simply dropped from the summations in the cost function and its gradient. Through the deliberate use of missing values one can implement certain extensions of MDS such as multidimensional unfolding (see Borg and Groenen (1997), chapter 14, in particular their Figure 14.1).

Missing values can be coded in the dissimilarities file as “NA”, or they can be introduced through conditions that are under interactive control. Here is a symbolic description of the summation set of Stress and Strain:

$$I = \{ (i, j) \mid i \neq j, D_{i,j} \neq NA, T_0 \leq D_{i,j} \leq T_1, \text{Runif}(i, j) < \alpha, \dots \}$$

$$0 \leq T_0 \leq T_1, \text{ thresholds, defaults: } T_0 = 0, T_1 = \infty$$

$$\text{Runif}(i, j) = \text{uniform random numbers} \in [0, 1].$$

$$\alpha = \text{selection probability, default: } \alpha = 1.$$

$$\dots = \text{conditions based on color/glyph groups.}$$

Here are details on removal conditions under interactive control:

- **Thresholding:** The lower and upper threshold parameters  $T_0$  and  $T_1$  for the conditions  $T_0 \leq D_{i,j} \leq T_1$  can be interactively controlled (by grips under the histogram in the X/GGvis control panel, on the left in Figure 3). Thresholding can be used to check the influence of large and small dissimilarities by removing them. We implemented these operations based on the received wisdom that the global shape of MDS configurations is mostly determined by the large dissimilarities. This statement is based on a widely cited study by Graef and Spence (1979) who ran simulations in which they removed,

respectively, the largest third and the smallest third of the dissimilarities. They found devastating effects when removing the largest third, but relatively benign effects when removing the smallest third. With interactive thresholding the degree to which this behavior holds can be explored for every dataset individually.

- **Random selection** is implemented by thresholding uniform random numbers  $\text{Runif}(i, j)$ . The condition  $\text{Runif}(i, j) < \alpha$  removes the dissimilarity  $D_{i,j}$  with probability  $1 - \alpha$ . The selection probability  $\alpha$  can be controlled interactively. Because the selection is probabilistic, the number of selected dissimilarities is random. Repeatedly generating new sets of random numbers while optimization is continuously running, one gets a sense of how (un)stable the configuration is under random removal of dissimilarities. In our experience classical scaling does not respond well to the removal of even a small fraction of distances. Distance scaling is considerably more robust in this regard.

Another set of removal conditions for dissimilarities is based on color/glyph groups. Such groups can be entered from files or they can be generated interactively with brushing operations. We implemented the following ways of using groups in scaling:

- **Subsetting objects:** Remove some objects and scale the remaining objects. Removal is achieved by “hiding” color/glyph groups.
- **Within-groups scaling:** Remove the dissimilarities that cross color/glyph groups. This option can be useful for finding and comparing group-internal structure, which is often obscured in global configurations.

Within-groups scaling has slightly different behavior in classical and distance scaling: In classical scaling the groups are linked to each other by a common origin, but otherwise they are scaled independently. In distance scaling the groups can be moved independently of each other.

Note also that nonmetric scaling always introduces a certain dependence between groups because the isotonic transformation is obtained for the pooled within-groups dissimilarities, not for each group separately.

- **Between-groups scaling:** Remove the dissimilarities within the groups. Between-groups scaling with two groups is called multidimensional unfolding (Borg and Groenen 1997, chapter 14). Two groups is the case that is most prone to degeneracies because it removes the most dissimilarities. The more groups there are, the more dissimilarities are retained and hence stability is gained.
- **Anchored scaling:** The objects are divided into two subsets, which we call the set of anchors and the set of floaters. We scale the floaters by only using their dissimilarities with regard to the anchors. Floaters are therefore scaled individually, and their positions do not affect each other. The anchors affect the floaters but not vice versa. The configuration of the anchors is dealt with in one of two ways:
  - *Fixed anchors:* The anchors have a priori coordinates that determine their configuration. Such coordinates can be entered in an initial position file, or they

are obtained from previous configurations by manually moving the anchor points (with mouse dragging).

- *Scaled anchors*: The anchors have dissimilarities also. Configurations for the anchors can therefore be found by subjecting them to regular scaling. Internally scaling the anchors and externally scaling the floaters with regard to the anchors can be done in a single optimization (Section 6.3).

In our practice we usually start with scaled anchors. Subsequently we switch to fixed anchors. Then, while the optimization is running, we drag the anchor points into new locations in order to check the sensitivity and reasonableness of the configuration of the floaters.

The anchor metaphor is ours. Anchored scaling is called “external unfolding” in the literature (Borg and Groenen 1997, Section 15.1).

## 4.5 Weights

The cost functions are easily adapted to weights. We implemented weights that depend on two parameters, each for a different task:

$$w_{i,j} = D_{i,j}^r \cdot \begin{cases} w, & \text{if color/glyph of } i, j \text{ is the same} \\ (2 - w), & \text{if color/glyph of } i, j \text{ is different} \end{cases}$$

$-4 \leq r \leq +4,$   $r = 0$  : ignore dissimilarities (default)  
 $r = -1$  : Sammon’s mapping  
 $0 \leq w \leq 2,$   $w = 1$  : ignore groups (default)  
 $w = 2$  : within-groups scaling  
 $w = 0$  : between-groups scaling

The first factor in the weights can depend on a power  $r$  of the dissimilarities. If  $r > 0$ , large dissimilarities are upweighted; if  $r < 0$ , large dissimilarities are downweighted. This is a more gradual form of moving small and large dissimilarities in and out of the cost function compared to lower and upper thresholding.

For metric distance scaling with  $r = -1$ , Sammon’s mapping (1969) is obtained, an independent rediscovery of a variant of MDS.

The second factor in the weights depends on groups: The parameter  $w$  permits continuous up- and downweighting of dissimilarities depending on whether they link objects in the same or different groups. This is a gradual form of moving between conventional scaling, within-groups scaling, and between-groups scaling. The latter are our ideas, while the weight-based gradual version is due to Priebe and Trosset (personal communication).

Note that weighting is computationally more costly than subsetting. The latter saves time because some dissimilarities do not need to be looked at, but weights are costly in terms of memory as we store them to save power operations in each iteration.

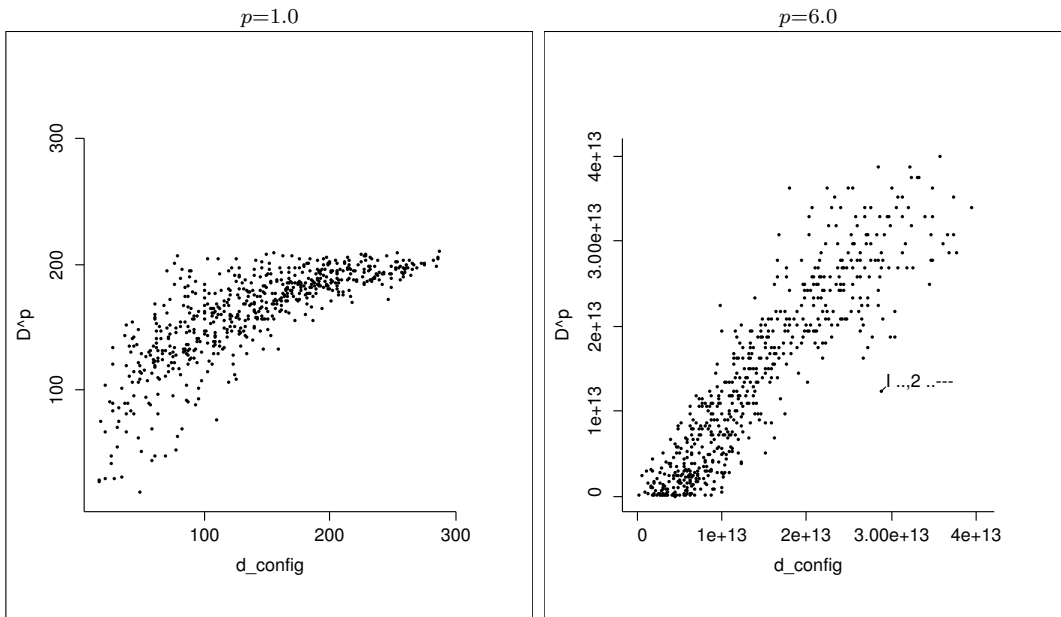


Figure 6: *Two Diagnostic Plots for Configurations from Metric Distance Scaling of the Morse Code Data. Left: raw data, power  $p = 1$ ; right: transformed data, power  $p = 6$ . An outlier is marked in the right hand plot: the pair of codes (1,2)  $\sim (\dots, \dots - - -)$  have a fitted distance that is vastly larger than the target dissimilarity.*

## 5 Diagnostics

A standard diagnostic in MDS is the Shepard plot, which is a scatterplot of the dissimilarities against the fitted distances, usually overlaid with a trace of the isotonic transform. See for example Borg and Groenen (1997, Sections 3.3 and 4.1) or Cox and Cox (1994, Section 3.2.4). The plot provides a qualitative assessment of the goodness of fit, beyond the quantitative assessment given by the Stress value.

The components for a Shepard plot are provided by X/GGvis on demand. The plot is part of a separate X/GGobi window which goes beyond a mere Shepard plot. The window contains seven variables:

- $d_{i,j}$ , the fitted quantities, which are  $\|\mathbf{x}_i - \mathbf{x}_j\|$  for distance scaling and  $\langle \mathbf{x}_i, \mathbf{x}_j \rangle$  for classical scaling (in which case the axis is labeled “b<sub>ij</sub>” rather than “d<sub>ij</sub>”),
- $f(D_{i,j})$ , the transformation of the dissimilarities, which is a power for metric scaling and an isotonic transformation for nonmetric scaling,
- $D_{i,j}$ , the dissimilarities,
- $r_{i,j} = f(D_{i,j}) - d_{i,j}$ , the residuals,
- $w_{i,j}$ , the weights, which may be a power of the dissimilarities,
- $i$ , the row index,

- $j$ , the column index.

Selecting the variables  $d_{i,j}$  and  $D_{i,j}$  yields the Shepard plot for distance scaling, and an obvious analog for classical scaling. Selecting  $D_{i,j}$  and  $f(D_{i,j})$  yields a plot of the transformation of the dissimilarities. Selecting  $d_{i,j}$  and  $f(D_{i,j})$  is possibly even more informative because the strength of the visible linear correlation is a qualitative measure for the quality of the fit. The right side of Figure 6 shows an example.

The residuals are provided for users who prefer residual plots over plots of fits. The weights are occasionally useful for marking up- and down-weighted dissimilarities with colors or glyphs. The row and column indices are useful for those X/GGvis modes in which dissimilarities have been removed from the Stress or Strain, or if some dissimilarities are missing. Plotting  $i$  versus  $j$  provides a graphical view of the missing and removal pattern of the dissimilarity matrix as it is used in the current cost function.

If the objects are given labels in an input file, the labels of the diagnostics window are pairs of object labels. In Figure 6, for example, an outlying point is labeled “I.,2.---”, showing two Morse codes, “..” for “I” and “.---” for “2”, whose dissimilarity is not fitted well.

## 6 Computational and Systems Aspects

### 6.1 Coordination and Linking of Windows

When starting up X/GGvis, two windows appear: the X/GGvis control panel and the X/GGobi window for the display of the configuration. A diagnostics window for the Shepard plot is created later at the user’s discretion.

Both the X/GGvis panel and its subordinate X/GGobi display live in the same process. As a result, the X/GGvis “master” and its X/GGobi “slave” can trivially share each other’s data. For example, the X/GGvis master is able to feed the X/GGobi slave the coordinates of the configurations at a fast pace so as to achieve algorithm animation. Similarly, the X/GGvis master is able to fetch the glyphs and colors from the X/GGobi slave in order to perform “within-groups MDS,” for example.

The window containing the configuration display is a complete X/GGobi window with all its capabilities for multivariate data visualization, including brushing and labeling (possibly linked to X/GGobi windows of covariates), data rotations (3-D rotations, grand tours and projection pursuit), parallel coordinate displays, and more (Swayne et al. 1998). We mentioned manually moving points in Section 3: this capability works even when viewing data with 3-D rotations and higher-D grand tours, in which case motion in data space is performed parallel to the current projection plane, leaving the orthogonal backdimensions fixed.

The diagnostics window is a full X/GGobi window of its own. It is *not* linked to the configuration display. One can create diagnostics windows in arbitrary numbers and compare them with each other. The diagnostics window is a frozen snapshot and does not animate itself when X/GGvis performs optimization. The main reason for detaching the diagnostics

window from the rest of X/GGvis is that the size of its data is in the order  $N^2$  if the size of the configuration is  $N$ . A Shepard plot can hence get so large even for moderate  $N$  that the system would slow down to an intolerable degree if animation were attempted. It is, however, useful to always show the current number of dissimilarities and update it continuously when operations are performed that remove or add dissimilarities.

## 6.2 Optimization and Interactivity

For minimization of Stress and Strain we mostly follow Kruskal’s (1964b) gradient method. This choice was based on the simplicity with which gradient methods generalize to cost functions with arbitrary weights and non-Euclidean Minkowski metrics. An additional argument could be derived from evidence that the more popular SMACOF algorithm (Borg and Groenen 1997, and references therein) may suffer from premature stopping or stopping at stationary rather than locally optimal solutions (Kearsley, Tapia and Trosset, 1998).

For metric scaling, Kruskal’s method is plain gradient descent on the cost function with regard to the configuration. For nonmetric scaling, Kruskal’s method consists of alternation between gradient descent on the configuration and estimation of the isotonic transformation. The latter is based on a convex least squares problem that can be solved with Kruskal’s pool-adjacent-violators algorithm.

An important part of Kruskal’s method is a stepsize strategy. This, however, we do not use because we submit the stepsize to interactive user control. It is scaled in relation to the size of the configuration such that, for example, a stepsize of 0.05 means that the gradient is 5% the size of the configuration, where size of the configuration and the gradient is measured as the sum of the distances from their respective mean vectors.

As we indicated earlier (Section 3), we do not provide automated stopping criterion either: the system runs a gradient descent loop until the user stops it interactively. An advantage of interactive over automated stopping is that non-trivial local movement in the configuration may still be visually apparent even when the descent in the cost function has become negligible. Another advantage is enabling the “fluid mode of operation” in which the user is free to manipulate configurations and parameters without having to restart optimization after every manipulation (Section 3).

## 6.3 Gradient Descent on the Configuration and Force Graphs

We now focus on details of the gradient descent step with a fixed transformation. The goal is to bring conventional MDS and anchored MDS (Section 4.4) into a single computational framework. The derivations may seem somewhat technical but there is reward in the clarity achieved.

We first note that minimizing Stress and Strain is equivalent to maximizing the respective cosine expressions of Sections 4.1 and 4.2. Omitting terms that do not depend on the

configuration, we are to maximize a ratio of the following form:

$$\frac{Num}{Denom} = \frac{\sum_{(i,j) \in I} w_{i,j} \cdot g(D_{i,j}) \cdot s(\mathbf{x}_i, \mathbf{x}_j)}{\left(\sum_{(i,j) \in I} w_{i,j} \cdot s(\mathbf{x}_i, \mathbf{x}_j)^2\right)^{1/2}}, \quad (2)$$

where  $s(\mathbf{x}_i, \mathbf{x}_j)$  is a Minkowski distance (to the  $q$ 'th power) for distance scaling, and the inner product for classical scaling. Both, distances and inner products, are symmetric in their arguments, hence  $s(\mathbf{x}_i, \mathbf{x}_j)$  is symmetric in  $i$  and  $j$ . As  $D_{i,j}$  is assumed symmetric in the subscripts, so is  $w_{i,j}$ .

The gradient of the ratio with regard to the configuration  $\mathbf{X} = (\mathbf{x}_i)_{i=1..N}$  is the collection of *partial gradients* with regard to configuration points  $\mathbf{x}_i$ :

$$\frac{\partial}{\partial \mathbf{X}} \frac{Num}{Denom} = \left( \frac{\partial}{\partial \mathbf{x}_i} \frac{Num}{Denom} \right)_{i=1..N}.$$

Because we determine the size of gradient steps as a fraction of the size of the configuration, we only need the partial gradients up to a constant factor:

$$\frac{\partial}{\partial \mathbf{x}_i} \frac{Num}{Denom} \propto \sum_{j \in \{j | (i,j) \in I\}} w_{i,j} \left( g(D_{i,j}) - \frac{Num}{Denom^2} s(\mathbf{x}_i, \mathbf{x}_j) \right) \frac{\partial}{\partial \mathbf{x}} \Big|_{\mathbf{x}=\mathbf{x}_i} s(\mathbf{x}, \mathbf{x}_j), \quad (3)$$

In the derivation of this formula we used symmetry of  $D_{i,j}$ ,  $w_{i,j}$ ,  $s(\mathbf{x}_i, \mathbf{x}_j)$ , and also symmetry of the set  $I$ , that is,  $(i,j) \in I \Rightarrow (j,i) \in I$ . The summation should really extend over the set

$$\{j | (i,j) \in I \text{ or } (j,i) \in I\},$$

but if  $I$  is symmetric it is sufficient to sum over the reduced set

$$\{j | (i,j) \in I\}.$$

Reduced summation lends an intuitive interpretation to partial gradients: The summand indexed by  $j$  is the contribution of  $\mathbf{x}_j$  to the gradient movement of the point  $\mathbf{x}_i$ . As such, it can be interpreted as the “force” exerted by  $\mathbf{x}_j$  on  $\mathbf{x}_i$ . The reduced summation means that under the symmetry assumptions it is sufficient to consider the force exerted by  $D_{i,j}$  on  $\mathbf{x}_i$  only, although strictly speaking both  $D_{i,j}$  and  $D_{j,i}$  exert force.

We now elaborate on the implications of reduced summation when it is carried over to certain types of non-symmetric sets  $I$ . First we re-interpret gradient computation with reduced summation by noting that it really produces the gradient of another criterion that is conceptually different from the above ratio (2). To see this, we introduce “bimodal” Stress/Strain, or a “bimodal” ratio analogous to the “unimodal” ratio (2), as follows:

$$\frac{Num}{Denom}(\xi_1, \dots, \xi_N | \mathbf{x}_1, \dots, \mathbf{x}_N) = \frac{\sum_{(i,j) \in I} w_{i,j} \cdot g(D_{i,j}) \cdot s(\xi_i, \mathbf{x}_j)}{\left(\sum_{(i,j) \in I} w_{i,j} \cdot s(\xi_i, \mathbf{x}_j)^2\right)^{1/2}} \quad (4)$$

We note:

- The reduced-summation gradient (3) is exactly the plain gradient of (4) with regard to the  $\xi_i$ 's at  $\xi_i = \mathbf{x}_i \forall i$ .
- Maximizing (4) with regard to the  $\xi_i$ 's given fixed  $\mathbf{x}_j$ 's amounts to anchored scaling with fixed anchors  $\{\mathbf{x}_1, \dots, \mathbf{x}_N\}$  and floaters  $\{\xi_1, \dots, \xi_N\}$ .

The first point assures that gradient steps based on (3) with reduced summation do find local maxima of the “unimodal” criterion (2) when the summation set  $I$  is symmetric. The second point hints that we should be able to incorporate anchored scaling by searching for local maxima of the bimodal ratio (4) if we use suitable summation sets  $I$  that are *not* symmetric.

We illustrate this point with an example. Consider a dissimilarity matrix whose first column is missing:  $D_{i,1} = NA \forall i$ , or equivalently,  $I = \{(i, j) \mid 1 \leq i \leq N, 2 \leq j \leq N\}$ . The missing first column means that  $\mathbf{x}_1$  does not contribute to the partial gradient (3) of any point whatsoever, but its own partial gradient has contributions from those points for which  $D_{1,j}$  is not missing. Intuitively,  $\mathbf{x}_1$  does not exert force but it “feels” force from other points; it does not “push”, but it is being “pushed”. In other words,  $\mathbf{x}_1$  is a floater, and its anchors are  $\{\mathbf{x}_j \mid D_{1,j} \neq NA\}$ . This example shows that a suitable  $NA$  pattern in the dissimilarities permits us to implement anchored scaling in addition to conventional scaling.

We discuss briefly the  $NA$  patterns of the group-based scaling methods of Section 4.4:

- Within-groups scaling, illustrated with two groups:

$$D = \begin{array}{cc} \text{group1} & \text{group2} \\ \left( \begin{array}{cc} D_{grp1,grp1} & NA \\ NA & D_{grp2,grp2} \end{array} \right) & \begin{array}{l} \text{group1} \\ \text{group2} \end{array} \end{array}$$

Group 1 gets scaled internally, and so does group 2. The forces are confined within the groups. The summation set  $I$  is symmetric.

- Between-groups scaling, illustrated with two groups (multidimensional unfolding):

$$D = \begin{array}{cc} \text{group1} & \text{group2} \\ \left( \begin{array}{cc} NA & D_{grp1,grp2} \\ D_{grp2,grp1} & NA \end{array} \right) & \begin{array}{l} \text{group1} \\ \text{group2} \end{array} \end{array}$$

The two groups exert force on each other, but there is no force within the groups. The summation set  $I$  is again symmetric.

- Anchored scaling with scaled anchors (a form of external unfolding):

$$D = \begin{array}{cc} \text{anchors} & \text{floaters} \\ \left( \begin{array}{cc} D_{ancr,ancr} & NA \\ D_{fltr,ancr} & NA \end{array} \right) & \begin{array}{l} \text{anchors} \\ \text{floaters} \end{array} \end{array}$$

Here the summation set  $I$  is no longer symmetric. The top left submatrix causes conventional scaling of the anchors. The bottom left submatrix exerts the push of the anchors on the floaters. The two blocks of  $NA$ 's on the right imply that the columns for the floaters are absent, that is, the floaters do not push any points.

- Anchored scaling with fixed anchors (another form of external unfolding):

$$D = \begin{array}{cc} & \begin{array}{cc} \text{anchors} & \text{floaters} \end{array} \\ \begin{pmatrix} NA & NA \\ D_{fltr,ancer} & NA \end{pmatrix} & \begin{array}{c} \text{anchors} \\ \text{floaters} \end{array} \end{array}$$

Again the summation set  $I$  is not symmetric. The two top blocks of  $NA$ 's imply that the anchors are fixed: they are not being pushed by anyone. The only push is exerted by the anchors on the floaters through the matrix on the bottom left.

It becomes clear that  $NA$  patterns and the corresponding summation sets  $I$  form a language for expressing arbitrarily complex constellations of forces. This idea can be formalized in terms of what we may call a “force graph”, defined as the directed graph with nodes  $\{1, \dots, N\}$  and edges in the summation set

$$I = \{(i, j) \mid D_{i,j} \neq NA\} .$$

An edge  $(i, j)$  stands for “ $j$  pushes  $i$ ”. Conventional MDS is represented by a complete graph, where every point pushes every other point. For within-groups scaling the force graph decomposes into disconnected complete subgraphs (cliques). Between-groups scaling has a complete bi-directional, multi-partite graph, that is, the node set is decomposed into two or more disjoint partitions, and the edge set is the set of edges from any one partition to any other. Anchored MDS with fixed anchors has a uni-directional complete bipartite graph, that is, the two partitions have asymmetric roles in that the edges go only from one of the partitions to the other. In anchored MDS with scaled anchors, the latter form in addition a clique. One can obviously conceive of more complex force graphs, such as multi-partite graphs with layered anchoring, or graphs with selected force cycles, but this is not the place to pursue the possibilities in detail.

## 6.4 MDS on Large Numbers of Objects

MDS is based on  $N^2$  algorithms, a fact that limits its reach for large  $N$ . On the hardware at our disposal, interactive use of X/GGvis is possible up to about  $N = 1000$ . Larger  $N$  can be processed also, but the user will leave the optimization to itself for a while. The largest  $N$  we have scaled with X/GGvis was  $N = 3648$ , but still larger  $N$  are feasible with more patience.

Among the four types of MDS, the nonmetric varieties are never recommended for  $N$  greater than a few hundred because setting up the isotonic regression adds initially a considerable computational burden. Among the two metric varieties, classical scaling is faster than

distance scaling. It is therefore a common strategy to use classical scaling solutions as initial configurations for distance scaling. For what it's worth, on a laptop computer with model year 2000 the dimension reduction example of Section 7 with  $N = 1926$  required about 5 seconds per gradient step for metric distance scaling and under 4 seconds per step for metric classical scaling.

We mentioned in Section 4.5 that weighted MDS is costly. When  $N$  is large, one should abstain from the use of weights for space reasons. We do not allocate a weight array if the weights are identical to 1.

The reach of MDS extends when a substantial number of terms is trimmed from the Stress function. Such trimming is most promising in anchored MDS (Section 4.4), which can be applied if an informative set of anchors can be found. The choice of anchors can be crucial; in particular, a random choice of anchors often does not work. But we have had success with the example of size  $N = 3648$  mentioned earlier: satisfying configurations were found with an anchor set of size 100, which reduced the time needed for a single gradient step from 100 seconds to 6 seconds.

## 7 Examples of MDS Applications

We give some data examples that demonstrate the wide applicability of MDS and the usefulness of X/GGvis.

- **Distance data of computer usage:** As part of a project on intrusion detection at AT&T Labs (Theus and Schonlau 1998), users were characterized by their logs of operating system commands that they typed during a number of work days. From each log, pairs of commands were characterized by a dissimilarity value that measured how far spaced in time the commands were used on average. Each dissimilarity matrix was considered as the signature of a user. MDS was used to create 2-D maps of the commands for a particular user. Two examples are shown in Figure 7. One user was a member of technical staff, the other an administrative assistant. The maps differ in characteristic ways, and they have very intuitive meanings in terms of general activities such as start up at the beginning of the day, e-mailing, programming, word processing.
- **Dimension reduction:** From a multivariate dataset with eight demographic and telephone usage variables for 1926 households we computed a Euclidean distance matrix after standardizing the variables. MDS was used to reduce the dimension from eight to two by creating a 2-D map. Figure 8 shows the result, side by side with a 2-D principal component projection. While MDS squeezes 20% more variance into two dimensions than PCA, its map shows rounding on the periphery that may be artifactual. This defect, combined with vastly greater computational cost, convinced us that MDS cannot be generally recommended for dimension reduction.
- **Layout of telephone call graphs:** The development of XGvis was originally motivated by the problem of laying out graphs in more than two dimensions and using

XGobi as a display device (Littman et al. 1992). In order to lay out a graph with MDS, one computes from the graph a distance matrix that can be subjected to MDS, such as the “shortest-path metric”. X/GGvis accepts graphs as input data, represented as a list of pairs of object numbers, and it computes the shortest-path metric at start-up. It also represents the graph visually with lines connecting configuration points. Figure 9 shows an example of a call graph with 110 nodes.

- **Molecular Conformation:** This is the task of embedding molecules in 3-D based on partial information about the chemical bonds. We give a somewhat unusual example that really amounts to a graph layout: D. Asimov (1998) devised a method for describing all possible capped nanotubes. His construction produces graphs with carbon atoms as nodes and bonds as edges. We show the graph layout of one such nanotube in Figure 10. Although the shortest-path metric of this molecular graph is far from Euclidean, the embedding is quite acceptable and certainly an excellent start for a more specialized chemical bond optimizer.

## 8 Conclusions

This article hoped to accomplish the following:

- To give an introduction to multidimensional scaling from the point of view of interactive data visualization.
- To describe functionality of systems, X/GGvis, that act as test beds for exploring the reach of human control in MDS computations.
- To outline an extensive set of tools for creating, visualizing, manipulating and diagnosing MDS configurations.
- To give a selected tour of MDS applications.

We finally refer the interested reader to a companion paper (Buja and Swayne 2002) for MDS methodology that is supported by the functionality described in this article.

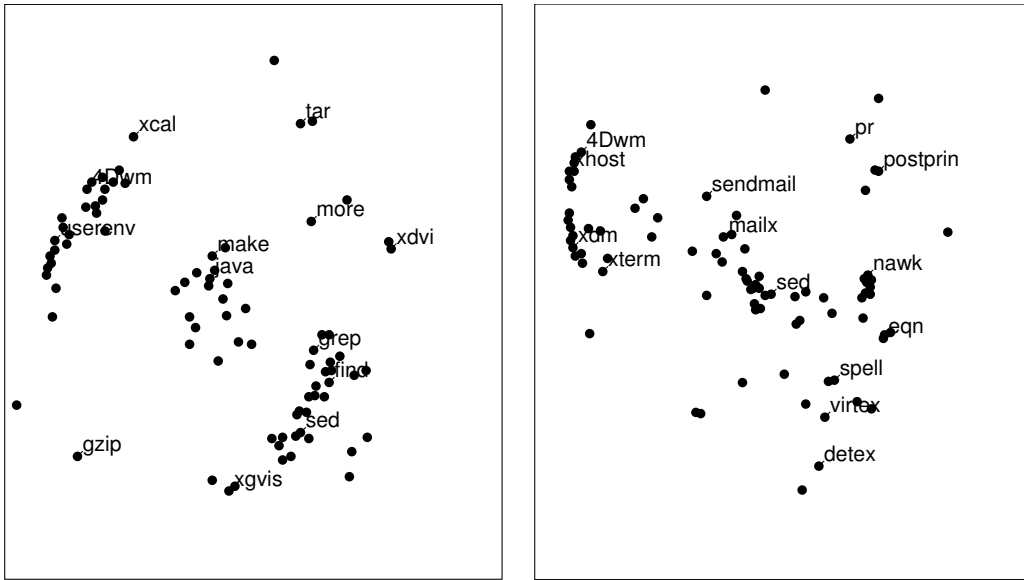


Figure 7: *Maps of Computer Commands for Two Individuals.*  
 Left: a member of technical staff who programs and manipulates data (Stress=0.29).  
 Right: an administrative assistant who does e-mail and word processing (Stress=0.34).

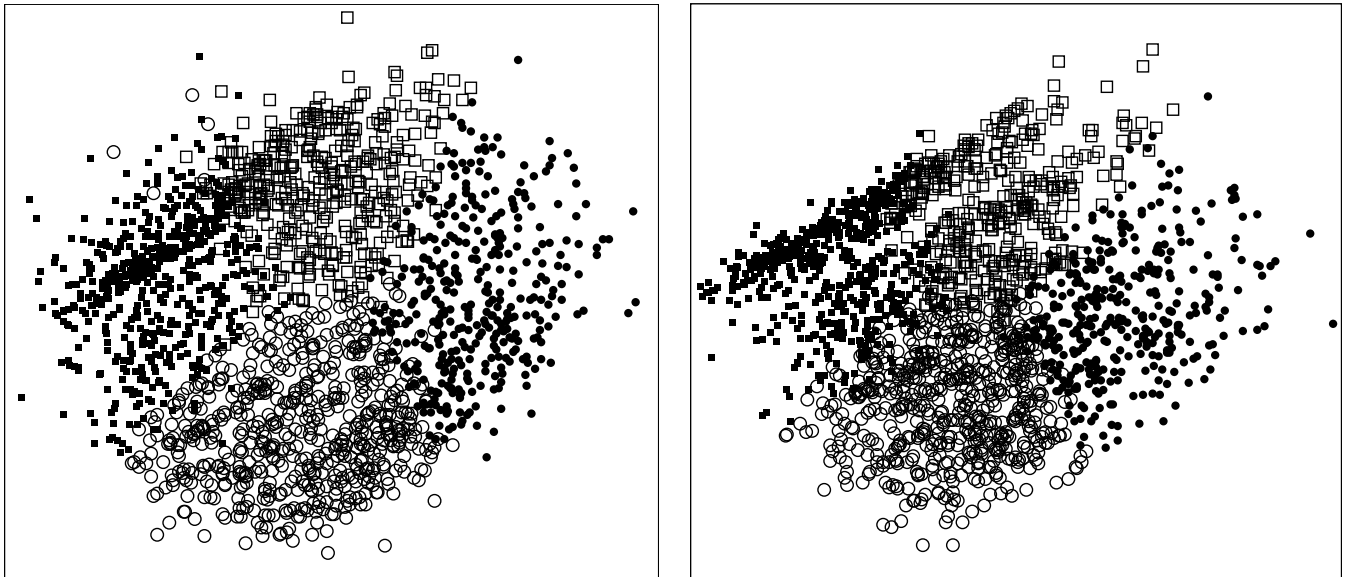


Figure 8: *Marketing Segmentation Data.* Left: MDS reduction to 2-D; right: largest two principal components. The glyphs represent four market segments constructed with k-means clustering using four means.

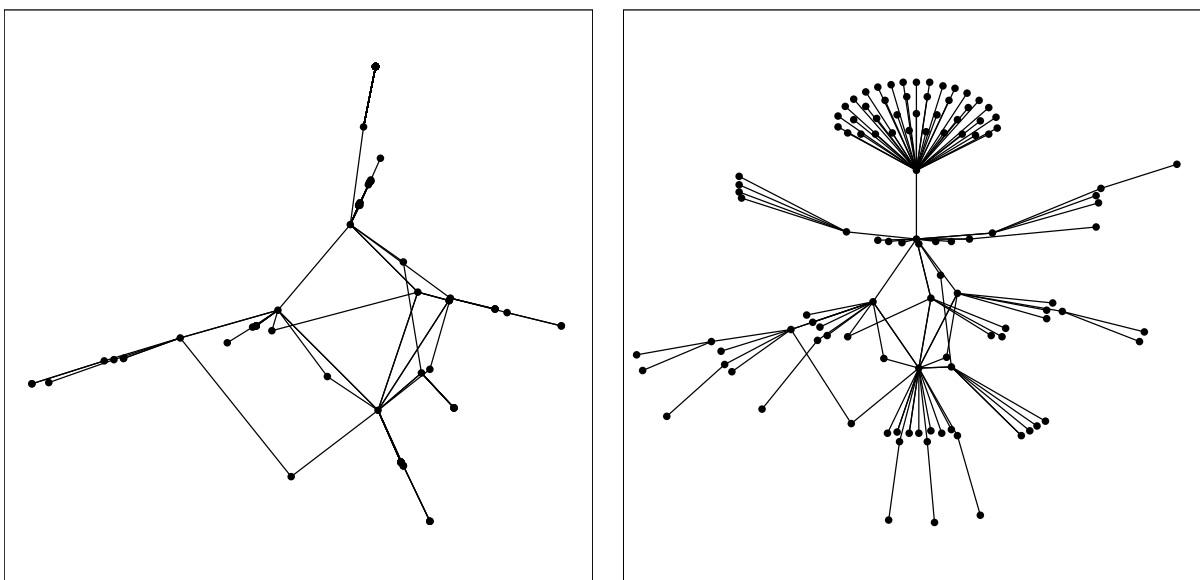


Figure 9: A Telephone Call Graph, Layed Out in 2-D. Left: classical scaling ( $Stress=0.34$ ); right: distance scaling ( $Stress=0.23$ ). The nodes represent telephone numbers, the edges represent the existence of a call between two telephone numbers in a given time period.

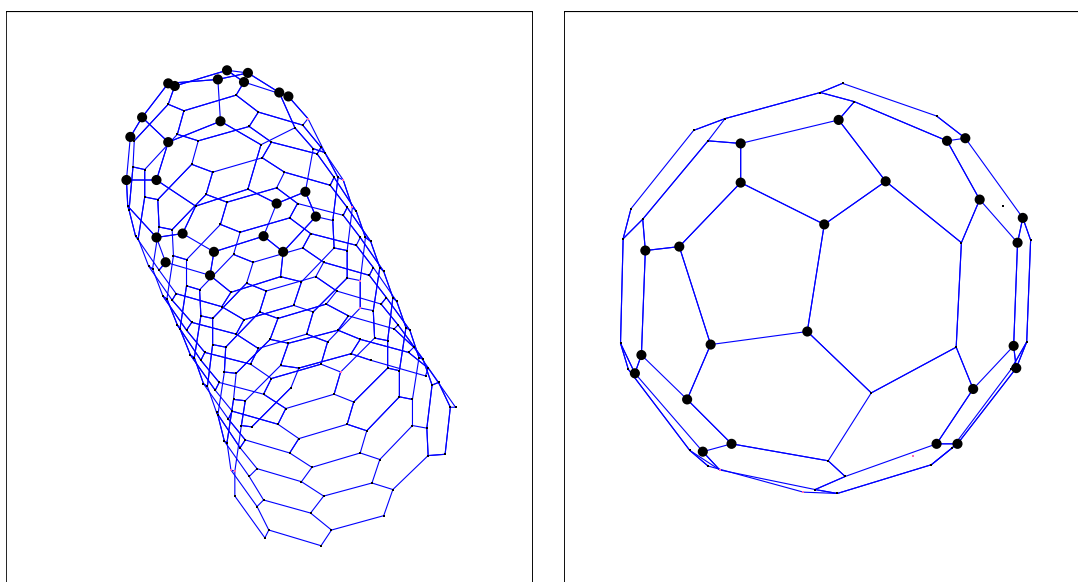


Figure 10: Nanotube Embedding. One of Asimov's graphs for a nanotube is rendered with MDS in 3-D ( $Stress=0.06$ ). The nodes represent carbon atoms, the lines represent chemical bonds. The right hand frame shows the cap of the tube only. Some of the pentagons are clearly visible.

# Acknowledgments

We thank Jon Kettenring and Daryl Pregibon, the two managers who made this work possible. We are indebted to Brian Ripley for his port of the XGvis/XGobi to Microsoft Windows<sup>TM</sup>. We also thank an associate editor and a reviewer for extensive comments and help with scholarship.

# References

- [1] Asimov, D. (1998), “Geometry of Capped Nanocylinders,” AT&T Labs Technical Memorandum, <http://www.research.att.com/areas/stat/nano>
- [2] Borg, I., and Groenen, P. (1997), *Modern Multidimensional Scaling: Theory and Applications*, New York: Springer-Verlag.
- [3] Buja, A., Cook, D., and Swayne, D. F. (1996), “Interactive high-dimensional data visualization,” *J. of Computational and Graphical Statistics*, **5**, pp. 78–99.
- [4] Buja, A., and Swayne, D. F. (2002), “Visualization Methodology for Multidimensional Scaling,” *J. of Classification*, **19**, pp. 7-43.
- [5] Cox, R. F., and Cox, M. A. A. (1994), *Multidimensional Scaling*, London: Chapman & Hall.
- [6] Crippen, G. M., and Havel, T. F. (1978), “Stable calculation of coordinates from distance information,” *Acta crystallographica*, **A34**, pp. 282-284.
- [7] Di Battista, G., Eades, P., Tamassia, R. and Tollis, I. (1994), “Algorithms For Drawing Graphs: An Annotated Bibliography,” *Computational Geometry*, **4**, pp. 235-282.
- [8] Glunt, W., Hayden, T. L., and Raydan, M. (1993), “Molecular conformation from distance matrices,” *J. of Computational Chemistry*, **14** 1, pp. 114-120.
- [9] Graef J., and Spence, I. (1979), “Using Distance Information in the Design of Large Multidimensional Scaling Experiments,” *Psychological Bulletin*, **86**, pp 60-66.
- [10] Havel, T. F. (1991), “An evaluation of computational strategies for use in the determination of protein structure from distance constraints obtained by nuclear magnetic resonance,” *Progress in Biophysics and Molecular Biology*, **56**, pp. 43-78.
- [11] Kearsley, A. J., Tapia, R. A., and Trosset, M. W. (1998), “The solution of the metric STRESS and SSTRESS in multidimensional scaling by Newton’s method,” *Computational Statistics*, **13**, pp. 369–396.

---

*Microsoft Windows* is a trademark of Microsoft, Inc.

- [12] Kruskal, J. B., and Wish, M. (1978), *Multidimensional Scaling*, Beverly Hills and London: Sage Publications.
- [13] Kruskal, J. B. (1964a), "Multidimensional scaling by optimizing goodness of fit to a nonmetric hypothesis," *Psychometrika*, **29**, pp 1-27.
- [14] Kruskal, J. B. (1964b), "Nonmetric multidimensional scaling: a numerical method," *Psychometrika*, **29**, pp. 115-129.
- [15] Kruskal, J. B., and Seery, J. B. (1980), "Designing Network Diagrams," *Proceedings of the First General Conference on Social Graphics, July 1980*, US Dept of the Census, Washington, DC, pp. 22-50.
- [16] Littman, M., Swayne, D. F., Dean, N., and Buja, A. (1992), "Visualizing the embedding of objects in Euclidean space," *Computing Science and Statistics*, **24**, pp. 208-217.
- [17] McFarlane, M., and Young, F. W. (1994), "Graphical Sensitivity Analysis for Multidimensional Scaling," *J. of Computational and Graphical Statistics*, **3**, pp. 23-33.
- [18] Meulman, J.J. (1992), "The integration of multidimensional scaling and multivariate analysis with optimal scaling," *Psychometrika*, **57**, pp. 539-565.
- [19] Rothkopf, E. Z. (1957), "A measure of stimulus similarity and errors in some paired-associate learning tasks," *J. of Experimental Psychology*, **53**, pp. 94-101.
- [20] Sammon, J. W., (1969), "A Non-Linear Mapping for Data Structure Analysis," *IEEE Trans. on Computers*, C-18(5).
- [21] Shepard, R. N. (1962), "The analysis of proximities: multidimensional scaling with an unknown distance function," I and II, *Psychometrika*, **27**, pp. 125-139 and pp. 219-246.
- [22] Swayne, D. F., Cook, D., and Buja, A. (1998), "XGobi: Interactive Data Visualization in the X Window System," *J. of Computational and Graphical Statistics*, **7**, pp. 113-130.
- [23] "Exploratory Visual Analysis of Graphs in GGobi," Swayne, D.F., Buja, A., Temple-Lang, D. (2003), proceedings of the *Third Annual Workshop on Distributed Statistical Computing* (DSC 2003), Vienna.
- [24] "GGobi: Evolving from XGobi into an Extensible Framework for Interactive Data Visualization," Swayne, D.F., Temple-Lang, D., Buja, A., and Cook, D. (2002), *Journal of Computational Statistics and Data Analysis*.
- [25] Takane, Y., Young, F. W. and De Leeuw, J. (1977), "Nonmetric individual differences multidimensional scaling: An alternating least-squares method with optimal scaling features," *Psychometrika*, **42**, pp 7-67.

- [26] Theus, M. and Schonlau, M., (1998), "Intrusion Detection Based on Structural Zeroes," *Statistical Computing & Graphics Newsletter*, **9**, pp 12-17. Alexandria, VA: American Statistical Association.
- [27] Torgerson, W. S. (1952), *Psychometrika*, **17**, pp. 401-419.
- [28] Trosset, M. W. (1998a), "Applications of Multidimensional Scaling to Molecular Conformation," *Computing Science and Statistics*, **29**, pp. 148-152.
- [29] Trosset, M. W. (1998b), "A New Formulation of the Nonmetric Strain Problem in Multidimensional Scaling," *J. of Classification*, **15**, pp. 15-35.